SURFACTANT ASSISTED HYDROTHERMAL SYNTHESIS OF ZINC SULFIDE NANOPARTICLES USING SINGLE SOURCE PRECURSORS

N. SHAHZAD[a], N. ALI[b,*], I. AHMAD[b], N. ULLAH[b], S. KHALID[c], M. FAZAL[a]
A. KALAM[d,e], A. G. AL-SEHEMI[d,e]
[a]National University of Sciences and technology (NUST), Pakistan
[b]Department of Physics, GPG Jahanzeb College Saidu Sharif, Swat, Pakistan, 19130
[c]National Centre for Physics, QAU campus, Islamabad, 43520, Pakistan
[d]Department of Chemistry, Faculty of Science, King Khalid University, Abha 61413, P.O. Box 9004, Saudi Arabia
[e]Research Center for Advanced Materials Science (RCAMS), King Khalid University, Abha 61413, P.O. Box 9004, Saudi Arabia

Lot of research is being carried out to develop solar cells which are economical with higher efficiencies. Many nanomaterials have been explored to tackle this issue. In this paper we have been used pure ZnS and cobalt doped ZnS nanoparticles which were hydrothermally synthesized from single source precursors using TX-100 as surfactant. The prepared precursors and samples were characterized using FTIR, TGA, XRD and UV-Visible. The crystallite size of the nanoparticles calculated from the XRD analysis have been found in the range of 20-25 nm. UV-Visible analysis at room temperature shows absorption peaks in the UV-region. The optical bandgap calculated using Tauc's plot from the absorption data lies in the region of 3.2-3.5 eV. This study helps in understanding novel performance of Co-ZnS in comparison to pure ZnS nanoparticles for its use in solar cell applications due to increase in photocatalytic activity in visible region.

1. Introduction

There are different forms of energy used in daily life namely, conventional and non conventional sources. Non conventional sources include solar, wind, tidal bio energy etc. Conventional sources of energy or (Non-renewable sources of energy) are those sources which are used one time or we cannot use it once they are used. Among these petroleum, coal and natural gas are Fossils fuels. Fossil fuels act as a source for the global energy requirement and there is continuous dependency on these which make them costly. A research conducted on the use of fossils fuels in 2013 shows that the world energy consumption[1] is 13,583 Mote (million tons of oil equivalent), which is increasing 2.3% /year from 2000 to 2013. This shows that the use of fossils fuels is increasing as these constitute approximately 88% of the energy consumption.

The world is facing massive energy crises, key cause being strong dependence on fossils-based fuels for energy generation for factories, industries and transportation system. The excessive use of fossils fuels is not only consuming our natural resources, which are limited but are also harmful to the environment i.e. (releasing the harmful gases CO_2, SO_2 etc.) since they act as a source of global warming and greenhouse effect. There are also a number of other factors which are the main cause of energy crises including; over consumption, poor infrastructure, over population, poor line distribution system, wars and attacks etc. Energy producing agents have strong influence on our surroundings. Coal, oil, Fossil fuels and natural gas produce maximum pollution and water contamination, loss of public health, injuring biota, loss of housing, land

---

* Corresponding author: nisar.ali@jc.edu.pk

contamination, and global warming etc. Conversely, renewable sources such as wind, solar, biogas and water have less damaging effect on environments and climate of our surroundings. Moreover, these sources will help us resolve the most critical issues like improved reliability of energy supply, ensuring sustainable development, ease implementation of the countries commitments with regards to International agreements [2].

The main energy sources are limited and the demand for it increasing day by day. To overcome this issue we have to explore new methods of production, which are renewable and environment friendly [3]. One of the answers to this solution can be solar energy instead of conventional sources of energies. i-e. oil, coal and natural gas [4].

Solar energy is environment friendly and does not produce any type of pollution, and can easily be converted to electrical energy by using photovoltaic solar cell.

This energy is free from any sort of pollutants or by products therefore it is called a main source of clean and green energy, and is available to every individual at any place [5]. Many researchers are of the opinion that one of the most viable solution to the energy crisis is harnessing of solar power. It is for this reason that the solar cells can be regarded as a mainstream renewable energy resource, if their design is economical and affordable as compared to other available renewable energy sources [6]. First and second generation solar cells are based on crystalline semiconductor and thin film structures having very less efficiencies although at lower costs. In order to overcome the low efficiency issue, new technologies are being researched without compromising the financial effects. It is for this reason that third generation of solar cells are based on nanotechnology, which is likely to cater for and enhance the efficiency issue thereby reducing the costs of the cells [6].

Chalcogenides are the compound of metals with Sulphur, selenium or tellurium, which are commonly used in glasses, crystals becasue their wide range of bandgap has established major part in optoelectronic devices[7]. The recent studies have shown that nanostructure chalcogenides are used as the effective component in the energy storage devices due to their distinctive chemical and physical properties[8]. Over the past year's transition, metal chalcogenides attracted much attention due to their vast application and interesting properties. Among all chalcogenides, metal sulfides have attracted more importance[9]. Metal sulfides (MSs) are significant group of minerals, showing diverse structural properties due to which it needs an elaborate study for investigation of its properties. In nature these substances are present abundantly, are cheap and exist as minerals, like chalcocite (Cu_2S), pyrite (FeS_2) and heazlewoodite (Ni_3S_2), and so on. Scientists have synthesized different metal sulfides in nano structures forms such as Cu_2S, Ni_3S_2, Co_9S_8 and ZnS etc. Of these (zinc sulfide) ZnS is a dominant semiconducting material having large excitation energy (~ 40 meV) and broad band gap (3.7 eV) due to which it is used as a multipurpose material. Having best properties or characteristics of luminesce these are used as an optical electronic device e.g. light emitting diodes, flat-panels displays and injection lasers etc. ZnS acts as a semiconducting photo-catalyst to eliminate toxic and organic water pollutants to the negative reduction potential of electron (excited) and a quick generation of holes-electron pairs[10].

Different techniques are established to prepare metal sulfides such as hydrothermal process, spry pyrolysis technique, chemical vapours deposition method, ultrasonic radiation, sol thermal method, co-precipitation, hot injection method, ligand exchange and vapor deposition method[11-20]. A brief synthesis of these techniques is tabulated in Table 1, 2 and 3. Zinc sulfide is a significant II-VI semiconductor which has been examined due to broad region of its applications. Zinc sulfide is chemically much stable than other chalcogenides due to which it is considered as a suitable host material. Zinc Sulfide has many applications ranging from optical to electrical and photodetector to photocatalysis. The current use of ZnS includes its use as an optical coating, optical sensors phosphors, and while in electrical properties, ZnS acts as a dielectric filter, field emission display and in LEDs. ZnS is polymorphous i.e. it exists in more than one crystalline form namely Zinc blend and wurtzite. The crystal geometry of zinc blend is cubic form "fcc" while wurtzite have hcp or hexagonal form[21].

Table 1. Synthesis of ZnS: methods and properties.

S No	Method	Reactants	Temperature	Advantages	Morphology	Ref
1	CBD	Thiourea, zinc salt in a basic solution with ammonia as complexing agent.	90 ℃	low cost and simple method	Thin film	[22]
2	Micro wave assisted method	zinc acetate and sodium sulfide reactants	140°C	less time consumption, particle size control,	ZnS Nano particle	[22]
3	Malt salt synthesis method	$Zn(NO_3)_2$ and Na_2S	200 °C	Single step, easy to scale-up, and cheap	hexagonal prism morphology	[2]
4	Spray pyrolysis method	metal nitrates and thio-urea $(SC(NH_2)_2$	600 °C.	inexpensive, simple,	Nano-sized zinc sulfide particles of 20–40 nm in diameter	[23]
5	Solvother-mal synthesis	hydrazine hydrate and acetic acid	110 °	low cost, energy efficient, low temperature processing, mild synthesis conditions, high yield phase purity	ZnS complex spheres	[24]
6	Hydrothermal method	bis(salicylaldiminato) zinc(II); $[Zn(sal)_2]$; and thioacetamide (CH_3CSNH_2).	105 °C	environmentally friendly technique	ZnS nanoclusters	[5]
7	Photo chemical method	Zn(CH3COO)2 and thiourea in presence of acetone		simple photochemical process easy to occur at room temperature	ZnS quantum dots	[25]
8	Single source precursor method	$Zn(cinnamtscz)_2$ and $ZnCl_2(cinnamtsczH)_2$	515 °C.	easier to control high purity side reactions can be restricted.	ZnS nanostructures	[26]
9	Thermal physical evaporation	Silicon wafer ZnS powder Argon	1000°C.	Structure uniform Nano rods with a thin amorphous surface	ZnS nanowires had a wurtzite-2 H type structure	[8]
10	Ultrasonic radiation	ZnO+Na2S+H2O	50 ∘C.	The product obtained is crystalline is compared to glassy structure	ZnS nanoparticles Size = 40nm	[14]
11	UV irradiation	isopropanol solution containing Zn(CH3COO)2 and thiourea in presence of acetone	20-25 ∘C.	Simple Occur at room temperature Controlled size Nano particles produced	Quantum Dots	[6]
12	Reverse micelle method	cyclohexane as an oil phase, Triton X-100 as a non-ionic surfactant and n-pentanol as a co-surfactant		Control size and shape Flexible reproducible safe and simple	3-5 nm ZnS NPs	[27]

Table 2. Synthesis of doped-ZnS: methods and properties.

S No	Dopants	Properties	Synthesis method used	Morphology	Band gap	Reason of doping	Size range (nm)	Ref.
1	Cu	Dialectics and conductivity increases.	chemical route method	Cubic, Nano clusters	Band gap decreases	→large Stokes shift →high thermal and chemical stability → long excited state.	2.9-3.6	[28]
2	Ni	Improved nonmagnetic property and conductivity decreases	chemical route method	Cubic, Nano clusters.	No description about band gap	-→ To improve the optical and electrical properties.	10.2	[29]
3	Cr	Broad emission band, Increasing dope- ng decrease emission into- misty.	chemical co-precipitation method	Cubic, nanoparticles	Decrease the band gap Depend on the dopants	-→to improve the optoelectronic devices. →effective PL and lasing in the mid IR spectral region.	9.5	[30]
4	Al	Al doping is used to decrease the resistivity	solution growth method	Cubic, Nano films/ sheets	Resistivity increases and band gap decreases	→wide application in photovoltaic especially used as a buffer/window layer.		[31]
5	Mn	Fluorescence bio imaging, also used	Hydrothermal method	Nano compo-site beads	Band gap varied with	→ for the photocatalytic-activity,	2.4± 0.3	[32]

S No	Dopants	Properties	Synthesis method used	Morphology	Band gap	Reason of doping	Size range (nm)	Ref.
		for detection of metal ions.			doping and increases with dopants	to increase the life time of photo generated Carriers.		
6	Au	Band gap decreases, increase photo response to the visible-light region.	Hydrothermal synthesis	Cubic Nano sheets	The band gap decreases	→ to improve the photo catalytic activity in the visible region	3.7-10	[33]
8	Co	Ferromagnetic, blue shift in optical activity	Colloidal chemical co-precipitation	Cubic, spherical sphere of diameter 39nm	Band gap increases	to Study the ferromagnetism and hysteresis loop.	35-39	[34]
9	Fe	Ferromagnetic, Show blue shift in absorption spectra.	Colloidal chemical co-precipitation method	Hexagonal, nanoparticles	Band increases with increase of dopants	To study the effects of dopants(Fe) on the ZnS and its optical ,magnetic, electric properties etc.	0.6-1	[35]
10	Ce	Blue shift in absorption spectra due to quantum confinement, bandgap decreases.	Hydrothermal method

solid state reaction method | Cubic, nanoparticle. Hexagonal nanoparticles | Bandgap increases. | To study quantum confinement effect and the properties changes due to this type of effect | 2nm

36 – 45 nm | [36, 37] |
11	Ga	Having wide doped, used for the nanoscale device integration	Electro chemical induction method	Composite nanotubes	Bandgap decreases	To make Ga doped ZnS nanowires, which further used for nanotube formation	25–30	[38]
12	Pd	Dilute magnetic properties,	Using Density functional theory by generalized gradient approximation	Cubic, Nanoparticles	Bandgap is varied	To make spintronic materials(which behave as a metal in one spin channel and an insulator in the other spin channel)	-	[39]
13	O	Improved optical properties.	DFT(Computational) model	Cubic and hexagonal structure	Bandgap changes	To increase the bulk and shear modulus, and appear new gaps.	-	[40]
14	Ag	Show quantum confinement effect. Blue shiftoccurs due to doping. Optical properties improved Band gap increases.	Thermal evaporation method	Zinc blende	Band gap increases	studied quantum confinement effect as the optical energy band gap increases significantly compared to the bulk ZnS.	in Nano range	[41]
15	In	Quantum size effects. Highly sensitive, to detect UV radiation.	Solve thermal methods.	Cubic,quantum dots Further analyze by DFT.	Band gap decreases	Highly selective absorption properties in the UV range. Redshift in absorption spectra	Nano range	[42]
16	Eu	Used in fabricating novel materials as well as in spintronic applications.	wet chemical method. Co-precipitation method.	Cubic. Quantum dots.	Band gap increases	To synthesis Eu doped ZnS QD,s which are Ferro magnetic in nature	Nano range	[43]
17	N	To fabricate single NR field-effect transistors,FETs	chemical vapor deposition method	Cubic symmetry, nanoribbons.		The resistivity of ZnS decreases with dopants.	Nano ribbons	[44]

Table 3. Co doped ZnS synthesis and properties.

S No	Dopants quantity	Synthesis method	Phase/Particles symmetry	Properties	Purpose of doping	Ref
1	0.2% to 10%	Phase thermal de-composition	Hexagonal, nanocrystals	Band gap decreases with increase of doping.	Enhancement of PV	[45]
2	0.1% 0.2% 0.3%	Co-precipitation	Cubic/ nanoparticles Size; 39nm	Blue shift occurs with increasing doping.	-------	[34]

S No	Dopants quantity	Synthesis method	Phase/Particles symmetry	Properties	Purpose of doping	Ref
3		Co-precipitation	Nanoparticles Size;1-4 nm	Highly stable. high dispersity of nanocrytallines systems.	Enhancement of PL and visible light emission	[46]
4	0.025 0.05	PLD is utilized for growing of thin films.	Thin film	Ferromagnetic material	Effects of dopants on magnetism	[47]
5		Spray pyrolysis technique	Thin film	Low average transmittance. Ban gap decreases. Ferromagnetic at room temp:	To study Optical, microstructural and magnetic properties	[48]
6	0.05	Solvo-thermal technique	Mesoporus Nano plate	High photosensitivity. High stability. High photo-catalytic activity.	To study the photocatalytic activity of Co-ZnS	[49]
7	1 to 6%	Chemical precipitation method	Cubic, nanoparticle	Band gap increases.	Effect of Co on the optical property of ZnS	[50]
8		Infrared irradiation method			To study the biological catalysis effect of Co-ZnS	[51]
9		Chemical precipitation method.	Nanoparticles; Size; 8-9nm	Band gap increases; 4.3Ev. PL emission enhanced in UV region.	To study the Nano phosphor Co-ZnS.	[52]
10	1 to 5%	Refluxing technique	Nanoparticles. Size; up to 10nm	Band gap increases.	To study the ferromagnetism and PL intensity	[53]
11	0.03% 0.05% 0.07% 0.1% 0.3%	Precipitation method	Nanosphere	Strong NBE emission And weak DL emission.	To study high quality ultraviolet material.	
12	UPTO 12%	CBD METHOD	Thin films	DFT is used	To study optical, magnetic properties od Co-ZnS	[54]
13	0.25 0.50 0.75	Theoretical approach using DFT.	-------	Electrical properties Structural properties. Magnetic properties.	Theoretical investigation of half metallicity in cobalt doped ZnS: DFT Studies.	[55]
14	UPTO 4.69%	Hydro-thermal method	Nano rods	Ferromagnetic Used in Nano scaled devices.	ferromagnetism and optical property of Zn1_xCoxS Nano rods	[56]
15	0.4%	Chemical deposition method	Thin film		Study the optical properties of Co-ZnS	[57]
16	0.02%	Hydro-thermal method	nanoparticles	Broad emission peak. High fluorescence efficiency.	study the different properties related to absorption, emission and transmittance spectra of Co-ZnS	[58]
17		Chemical solution deposition method	Cubic and hexagonal / nanoparticles		Studied: PL, quantum confinement effect, and synthetic method	[59]
18		Precipitation	Cubic.	Doped with Co and Cl. With increase in doping the absorption spectra increases	How to protect the ZnS from photo-corrosion	[60]
19		Hydro-thermal method.	Cubic/ NCs, NS, NN.	Different morphology will have different effect on electrolyte.	Effect of ZnS on Rechargeable Zinc air batteries	[61]
20		solvent-based sulfidation	47-1656/Hollow polyhedrons	excellent electro catalytic HER activity, highly stable in alkaline media. Highly efficient in PV.	Analysis of high-performance electro catalysts for the hydrogen evolution reaction	[62]
21		solvent-based sulfidation	47-1656/Hollow polyhedrons	excellent electro catalytic HER activity, highly stable in alkaline media. Highly efficient in PV.	Analysis of high-performance electro catalysts for the hydrogen evolution reaction	[63]
22		Hydro-thermal process	Nano sheets , leap like morphology.	May use as a sheet electrode in a superconductor.	Ternary ZnS	[64]
23		Hydro-thermal technique		Efficient photocatalytic activity. Used in hydrogen producing catalysis.	Analysis of the O_2 evolution by H_2O and H_2 generation by ammonia borane hydrolysis.	[65]

2. Materials and methods

All reagents used were of analytical grade. All the solutions were prepared in distilled water (E.C. 2.8μS/cm) which was obtained from the distillation apparatus (Model WSB/4, Hamilton Laboratory Glass Ltd.). All the chemicals used for the experiments were acquired from Sigma Aldrich with purity varying from 85% to 99%.

2.1. Synthesis of Zinc sulfide and Cobalt doped Zinc sulfide

Zinc sulfide nanoparticles have been prepared from single source precursor using zinc diethyldithiocarbamate (Zn-dtc). First Zn-dtc was first prepared from potassium hydro oxide (KOH) and DEA in the presence of CS_2 which was then used for the preparation of zinc sulfide. Similarly, Co-dtc was prepared by same method and afterwards doped with Zn-dtc with designed concentration to prepare cobalt doped zinc sulfide. The procedure followed for the synthesis was as per the study carried out by Khalid and co authors [66]. All the chemicals used were acquired from Sigma-Aldrich. In a common synthesis method, 0.3g(0.60mmol) of zinc precursor(1) and different mol% of dopant-precursor were used.

2.1.1. Synthesis of precursors

Zinc diethyldithiocarbamate Zn(DDTC) and cobalt diethyldithiocarbamate Co(DDTC) complexes were synthesized by the same procedure as published in the reference article[66]. The detailed synthesis procedures are as follow; Tris (N, N-diethyldithiocarbamate) zinc, $[Zn(S_2CN(Et)_2)_3]$. Potassium diethyldithiocarbamate was also synthesized as mentioned previously. In detail a mixture of potassium hydroxide (2g, 35.60 mmol) was stirred in ethanol (50ml) in a three/multi neck flask for twenty minutes . Then diethyl amine (3.68 ml, 35.6 mmol) was poured to the solution, and stirred continuously for thirty minutes. Then carbon disulfide (2.15ml, 35.6mmol) was poured drop wise slightly and stirred for 2-3 hours. Then a freshly synthesized solution of zinc nitrate monohydrate $(Zn(NO_3)_3\text{-}9H_2O)$ (2.96 g, 7.3 mmol) in 50ml ethanol was added slowly to the solution mixture with the help of dropping funnel. The overall reaction mixture was stirred for 5-6 hours. The end product obtained of white precipitate was filtered and washed, with ethanol water mixture and dried at normal atmospheric pressure.
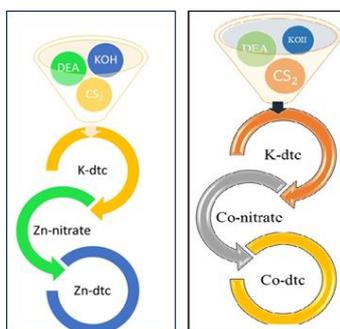

Fig. 1. Schematic diagram of Zn-dtc and Co-dtc preparation.

Tris (N.N.diethyldithiocarbamte) cobalt (2) was synthesized with similar procedure via cobalt nitrate hexahydrate ($Co(NO_3)_2\text{-}6H_2O$) (2.08 gm ,7.15 mmol) m.pt. 262-265 °C as shown in Fig. 1. Reaction schemes of ZnS and cobalt doped ZnS are shown in Figs. 2 and 3.

475

Fig. 2 Reaction scheme of ZnS.
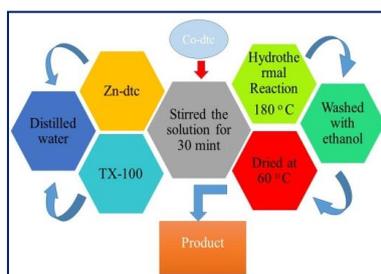
Fig. 3. Reaction scheme of cobalt doped ZnS.

2.2. Synthesis of Zinc sulfide by hydrothermal method using Zn(DDTC)

TX-100 was added drop wise in the 75% distilled water in 500 ml beaker and stirred solution for 20-30 minutes. After stirring the solution with magnetic stirrer 1 gm of Zn(DDTC) was added gently and stirred again for 30 minutes. The solution was then transferred to Teflon lined autoclave and closed properly with teflon cap. The autoclave was then placed in an oven already set at temperature 180 °C for three hours. After this, the oven was allowed to settle down to its room temperature, completing the reaction. The prepared solution was passed through the filter papers to get the desired product, which was then washed with ethanol 3-4 times. The product was then dried at 60 °C for 5 hours in oven. The final product thus obtained was then characterized for further analysis.

2.3. Synthesis of Cobalt doped zinc sulphide by hydrothermal method using Zn(DDTC)

Similar procedure was followed for preparing cobalt doped ZnS.   Drop wise TX-100 was added in the 75% of distilled water and stirred for 20-30 mint. After stirring 1 gm of Zn(DDTC) was added gently and stirred for another 30 mint . After a steady state of the solution 30 wt. % Co(DDTC) was added for its doping into Zn(DDTC). The above solution was added to Teflon autoclave properly closed with Teflon cap which was then placed in the oven already set at temperature 180 °C for three hours. The oven was then allowed to settle down to its room temperature completing the reaction. The prepared solution was passed through the filter papers to get the desired product, which was then washed with ethanol 3-4 times. The product was then dried at 60 °C for 5 hours in oven. The final product thus obtained was then characterized for further analysis.

3. Results and discussion

3.1. Thermal analysis

The thermal characterizations illustrate the temperature stability, decomposition temperature, thermo kinetics and the mass changes during reaction. The TGA shows insight information about decomposition and volatility by observing the weight loss verses temperature.

TGA analysis of Zn(dtc) and Co(dtc) are as shown in the Fig. 4 which illustrates that both the sample decompose in single step. Both the precursors show rapid weight loss between 220 °C to 340 °C and 240 °C to 380 °C and final residues remained are 14.6% and 14.90% as observed, respectively. The precursors on heating in nitrogen surrounding decompose to their corresponding metal sulfides.
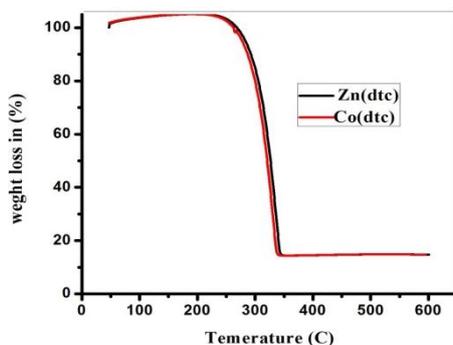

Fig. 4. Thermogravimetric analysis of Zn(dtc) and Co(dtc).

3.2. Fourier transform spectroscopy

The infrared spectra (IR) of complexes Zn(dtc) and Co(dtc) synthesized from KOH and diethyl amine (DEA) using the CS_2 as a medium were examined in the region 4000-400 cm^{-1}. The main spectrum showing the IR absorption due to different vibration modes are concisely discussed. The early spectrum ranges from 1475 to 1545 cm^{-1} describe thioureide (NCSS) band which characteristically happens between C-N and C=N band. The next section (1080-915 cm^{-1}) is expressive way of synchronization in dithiocarbamato moiety (CSS). The third region almost 345-395 cm^{-1} is ascribed to metal sulfide (Zn, Co-S) bonds. The (C—H) extending way for alkyl group is perceived in a range of 2910–2845 cm^{-1} although the C—H twisting happens as a strong bond near 1354 cm^{-1} in both precursors. The particular absorption in the area about 1005 cm^{-1} is the indication of symmetrically bonded or bidentate dithiocarbamate complexes. The region (1070-930 cm^{-1}) is the brief coordination mode of dithiocarbamato moiety. The region around (350-400) cm^{-1} shows the Zn-S and Co-S bond.
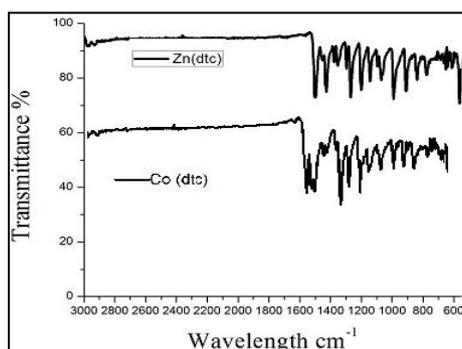

Fig. 5. FTIR spectra of Zn and Co(dtc).

3.3. Structure analysis

The structure verification and crystallinity of pure and cobalt doped ZnS nanoparticles fabricated by hydrothermal process via single source precursors were performed on x-ray diffraction. XRD analysis showed main five peaks corresponding to (100), (111), (101), (220) and (311) as shown in the figure 6. The pattern reveals the polycrystalline structure in which the three planes (111), (200) and (311) show the cubic planes (JCPDS# 001-0792), while the remaining two

(100) and (101) planes corresponding to wurtzite phase (JCPDS# 075-1534). Moreover, the dopant cobalt ion has no effect on the structure of ZnS nanoparticles, which indicate that cobalt ion is well incorporated in the ZnS lattice. Whilst a slight shift in angle is observed which increases with increase in angle. This shifting of peaks show the contraction in lattice which occurs when the zinc ions are substituted with cobalt ions, for the reason that the ionic radius of cobalt ion is smaller than that of the zinc ion. The average crystallite size was obtained from the full width at half maximum from the diffraction peaks using equation (A) is about 20nm for pure ZnS and 18nm for doped ZnS.
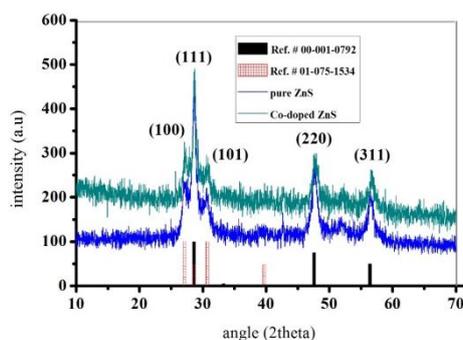
Fig. 6. XRD analysis of pure and Co doped ZnS.

3.4. UV-Visible spectroscopy

The optical properties of pure ZnS and cobalt doped ZnS have investigated. Figure 7 shows the UV-Visible absorption spectra of pure and cobalt doped ZnS. To observe absorption characteristics, the fabricated pure ZnS and cobalt doped nanoparticles are mixed with methanol solvent and placed in quartz cuvette in the UV-Visible spectrometer. The characteristics peaks of pure ZnS nanoparticles appear in the region of 250-400nm. The major excitonic peaks are present in between the 230-250nm. The pure ZnS show no absorption spectra in the region of 400-800nm. The cobalt doped ZnS show slightly blue shift due to the decrease of grain size and the increment of quantum size effect.

The principles absorption, which show the electronic excitation from the valence to conduction band are used to determine the characteristics band gap of the materials. The relation which relates the incident photon energy and absorption co-efficient is given by:

$$(\alpha h\nu)^{1/n} = A\ (h\nu - E_g)$$

The above equation shows the relation between band gap energy (E_g) and energy incident. Where A is constant, the 'n' depends on the type of transition whether it is direct or indirect for direct transition. For direct transition the 'n' is 2, while for indirect the 'n' is ½. The direct and indirect optical band gap for pure and doped ZnS is (3.1, 2.28eV) and (3.73, 3.46eV), respectively. The increase in bandgap is a result of small particle size as compared to pure ZnS.
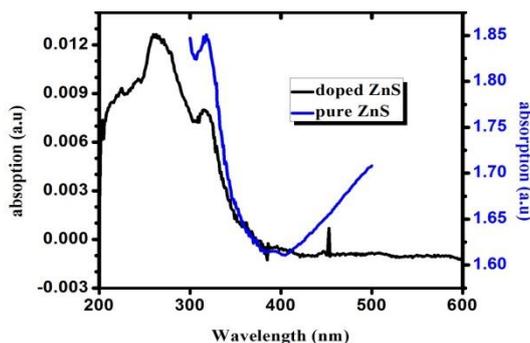
*Fig. 7. UV-Visible spectra of pure and Co-ZnS.*
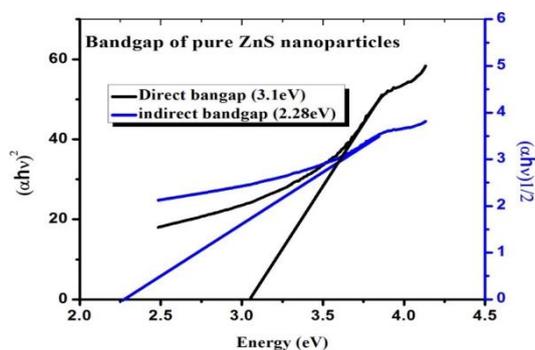

Fig. 8. Bandgap of pure ZnS.
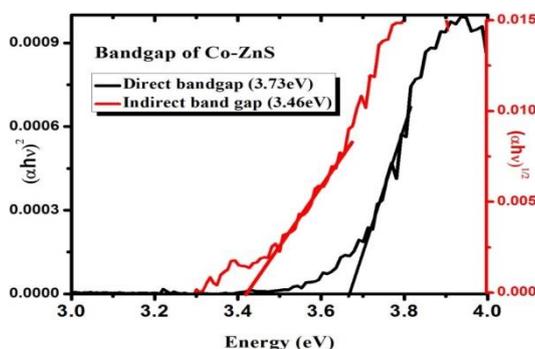
Fig. 9. Bandgap of cobalt doped ZnS.

4. Conclusion

ZnS acquired much interest due to its vast application in optoelectronic devices, photoluminescence, photocatalysis and biomedical compounds. Prominent work on the ZnS synthesis and assembling have been perceived in the last few years. The fundamental principles of synthesis and assembling is employed in changing ZnS in terms of morphology, structure and properties. In our report Pure ZnS and Co-ZnS nanoparticles were successfully synthesized from single source precursors by hydrothermal method using TX-100 as surfactant.

The chemical bonding and structural properties were characterized by FTIR and TGA, showing the purity of single source precursors. This method of synthesis is easy, accurate, low cost and easily assessable. The XRD analysis shows the diphase structure with a better crystallization, which demonstrates that the samples lattices are well generated having (20-25) nm crystallite size. The surfactant has strong hold on the surface of ZnS and depends on the reaction time. The UV-

visible shows the maximum absorption in the region of 300 nm while blue shift occurs with doping. The band gap also confirms the nanostructure of the materials.

Acknowledgement

References

[1] M. Zainol, N. Ismail, I. Zainol, A Review On The Status Of Tidal Energy Technology Worldwide **29**, 675 (2017).
[2] N. L. Panwar, S. C. Kaushik, S. Kothari, Renewable and Sustainable Energy Reviews **15**(3), 1513 (2011).
[3] E. D. Coyle, R. A. Simmons, Understanding the global energy crisis 2014: Purdue University Press.
[4] N. S. Lewis, D. G. Nocera, Proceedings of the National Academy of Sciences **103**(43), 15729 (2006).
[5] S. Sharma, K. K. Jain, A. Sharma, Materials Sciences and Applications **6**(12), 1145 (2015).
[6] Z. Abdin et al., Renewable and Sustainable Energy Reviews **26**, 837 (2013).
[7] P. K. Singh, D. Dwivedi, Ferroelectrics **520**(1), 256 (2017).
[8] M.-R. Gao et al., Chemical Society Reviews **42**(7), 2986 (2013).
[9] Y. Jiang et al., Journal of Solid State Chemistry **167**(1), 28 (2002).
[10] C.-H. Lai, M.-Y. Lu, L.-J. Chen, Journal of Materials Chemistry **22**(1), 19 (2012).
[11] A. Şahin, Hydrothermal synthesis and characterization of transition metal oxides, 2004, Izmir Institute of Technology.
[12] C. Falcony, M. Aguilar-Frutis, M. García-Hipólito, Micromachines **9**(8), 414 (2018).
[13] W. Bryant, Journal of Materials science **12**(7), 1285 (1977).
[14] J. Xu et al., Applied Physics A **66**(6), 639 (1998).
[15] G. Demazeau, Zeitschrift für Naturforschung B **65**(8), 999 (2010).
[16] P. Patnaik, Dean's analytical chemistry handbook. Vol. 1143. 2004: McGraw-Hill New York.
[17] D. Harvey, Modern analytical chemistry 2000: Boston: McGraw-Hill Companies, Inc.
[18] P. K. Santra et al., The journal of physical chemistry letters **4**(5), 722 (2013).
[19] B. Mao et al., The Journal of Physical Chemistry C **115**(18), 8945 (2011).
[20] O. Stroyuk, A. Raevskaya, N. Gaponik, Chemical Society Reviews, 2018.
[21] N. Kaur et al., J Bioelectron Nanotechnol. **1**(1), 5 (2016).
[22] A. Oliva et al., Chemical bath method for ZnS thin films preparation, 500 (2010).
[23] I. W. Lenggoro et al., Journal of Aerosol Science **31**(1), 121 (2000).
[24] L. Chai et al., Materials Letters **120**, 26 (2014).
[25] C. M. Gonzalez et al., Chemical Communications **51**(15), 3087 (2015).
[26] A. M. Palve, S. S. Garje, Bulletin of Materials Science **34**(4), 667 (2011).
[27] R. K. Whiffen et al., Journal of Luminescence **146**, 133 (2014).
[28] S. Ummartyotin et al., Solid State Sciences **14**(3), 299 (2012).
[29] H. Soni, M. Chawda, D. Bodas, Materials Letters **63**(9-10), 767 (2009).
[30] D. Amaranatha Reddy et al., Crystal Research and Technology **46**(7), 731 (2011).
[31] K. Nagamani et al., Current Applied Physics **12**(2), 380 (2012).
[32] W. Chen et al., Macromolecular Materials and Engineering, 2019.
[33] J. Zhang et al., ACS applied materials & interfaces **5**(3), 1031 (2013).
[34] S. Sambasivam et al., Journal of Solid State Chemistry **182**(10), 2598 (2009).
[35] S. Sambasivam et al., Materials Science and Engineering: B **150**(2), 125 (2008).

480

[36] K. V. Anand et al., International Journal of Nanoscience **10**(03), 487 (2011).
[37] L. Archana, D. N. Rajendran, Advanced Science Letters **24**(8), 5994 (2018).
[38] U. K. Gautam et al., Advanced Materials **20**(4), 810 (2008).
[39] J.-P. Tang et al., The European Physical Journal B **86**(8), 362 (2013).
[40] I. S. Popov, A. S. Vorokh, A. N. Enyashin, Chemical Physics **510**, 70 (2018).
[41] E. Shahriari et al., Optical and Quantum Electronics **49**(4),151 (2017).
[42] E. Della Gaspera et al., Nanoscale, 2019.
[43] S. Horoz et al., AIP Advances **6**(4), 045119 (2016).
[44] G. Yuan et al., Applied Physics Letters **93**(21), 213102 (2008).
[45] C. Bi et al., Materials Chemistry and Physics **116**(2-3), 363 (2009).
[46] R. Sarkar et al., Physica B: Condensed Matter **404**(21), 3855 (2009).
[47] S. P. Patel et al., Journal of Magnetism and Magnetic Materials **323**(22), 2734 (2011).
[48] I. Polat et al., Materials Chemistry and Physics **130**(1-2), 800 (2011).
[49] J. S. Jang et al., Applied Catalysis A: General **427**, 106 (2012).
[50] V. Ramasamy, K. Praba, G. Murugadoss, Spectrochimica Acta Part A: Molecular and Biomolecular Spectroscopy **96**, 963 (2012).
[51] A. Dandia et al., Journal of Molecular Catalysis A: Chemical **373**, 61 (2013).
[52] C. Pathak, M. Mandal, V. Agarwala, Materials Science in Semiconductor Processing **16**(2), 467 (2013).
[53] B. Poornaprakash et al., Journal of Alloys and Compounds **577**, 79 (2013).
[54] M. S. Akhtar et al., Journal of Materials Chemistry C **3**(26), 6755 (2015).
[55] M. S. Akhtar, S. Riaz, S. Naseem, Materials Today: Proceedings **2**(10), 5684 (2015).
[56] J. Yang et al., Superlattices and Microstructures **82**, 75 (2015).
[57] S. Kamble et al., Journal of Alloys and Compounds **656**, 590 (2016).
[58] B. Poornaprakash et al., Physica E: Low-dimensional Systems and Nanostructures **83**, 180 (2016).
[59] P. Asha, M. Rajeswari, B. Bindhu, Zinc sulfide nanoparticles: processing, properties and applications: an overview.
[60] P. Weide et al., Langmuir **32**(48), 12641 (2016).
[61] X. Wu et al., ACS applied materials & interfaces **9**(14), 12574 (2017).
[62] B. Zhang et al., Nanoscale **10**(4), 1774 (2018).
[63] W. Zhao et al., Journal of Alloys and Compounds **698**, 754 (2017).
[64] T. Y. Wei et al., Advanced materials **22**(3), 347 (2010).
[65] L. Qian, D. Jia, Y. Miao, Journal of The Electrochemical Society **166**(2), F18 (2019).
[66] S. Khalid et al., New Journal of Chemistry **39**(2), 1013 (2015).